

UCSF

UC San Francisco Previously Published Works

Title

The critically endangered vaquita is not doomed to extinction by inbreeding depression

Permalink

<https://escholarship.org/uc/item/31n8z5h6>

Journal

Science, 376(6593)

ISSN

0036-8075

Authors

Robinson, Jacqueline A
Kyriazis, Christopher C
Nigenda-Morales, Sergio F
[et al.](#)

Publication Date

2022-05-06

DOI

10.1126/science.abm1742

Supplemental Material

<https://escholarship.org/uc/item/31n8z5h6#supplemental>

Copyright Information

This work is made available under the terms of a Creative Commons Attribution License, available at <https://creativecommons.org/licenses/by/4.0/>

Peer reviewed

1 **Title: The critically endangered vaquita is not doomed to extinction by inbreeding**
2 **depression**

3

4 **Authors:** Jacqueline A. Robinson^{1*†}, Christopher C. Kyriazis^{2*†}, Sergio F. Nigenda-Morales³,
5 Annabel C. Beichman⁴, Lorenzo Rojas-Bracho^{5,6*}, Kelly M. Robertson⁷, Michael C. Fontaine^{8,9,10},
6 Robert K. Wayne², Kirk E. Lohmueller^{2,11*}, Barbara L. Taylor^{7*}, and Phillip A. Morin^{7*}

7

8 **Affiliations:**

9 ¹Institute for Human Genetics, University of California, San Francisco; San Francisco, CA, USA.

10 ²Department of Ecology and Evolutionary Biology, University of California, Los Angeles; Los
11 Angeles, CA, USA.

12 ³Advanced Genomics Unit, National Laboratory of Genomics for Biodiversity (Langebio), Center
13 for Research and Advanced Studies (Cinvestav); Irapuato, Guanajuato, Mexico.

14 ⁴Department of Genome Sciences, University of Washington; Seattle, WA, USA.

15 ⁵Comisión Nacional de Áreas Naturales Protegidas/SEMARNAT; Ensenada, Mexico.

16 ⁶PNUD-Sinergia en la Comisión Nacional de Áreas Naturales Protegidas, Ensenada, B.C.,
17 México.

18 ⁷Southwest Fisheries Science Center, National Marine Fisheries Service, NOAA ; La Jolla, CA,
19 USA.

20 ⁸MIVEGEC, Université de Montpellier, CNRS, IRD; Montpellier, France.

21 ⁹Centre de Recherche en Écologie et Évolution de la Santé (CREES); Montpellier, France.

22 ¹⁰Groningen Institute for Evolutionary Life Sciences (GELIFES), University of Groningen;
23 Groningen, The Netherlands.

24 ¹¹Department of Human Genetics, David Geffen School of Medicine, University of California, Los
25 Angeles; Los Angeles, CA, USA.

26

27 *Correspondence: jacqueline.robinson@ucsf.edu, ckyriazis@g.ucla.edu,
28 lrojasbracho@gmail.com, barbara.taylor@noaa.gov, klohueller@g.ucla.edu,
29 phillip.morin@noaa.gov

30

31 †Contributed equally

32

33 **Abstract:** In cases of severe wildlife population decline, a key question is whether recovery
34 efforts will be impeded by genetic factors such as inbreeding depression. Decades of excess
35 mortality from gillnet fishing have driven Mexico's vaquita porpoise (*Phocoena sinus*) to ~10
36 remaining individuals. We analyzed whole genome sequences from 20 vaquitas and integrated
37 genomic and demographic information into stochastic, individual-based simulations to quantify
38 the species' recovery potential. Our analysis suggests the vaquita's historical rarity has resulted
39 in a low burden of segregating deleterious variation, reducing the risk of inbreeding depression.
40 Similarly, genome-informed simulations suggest the vaquita can recover if bycatch mortality is
41 immediately halted. This study provides hope for vaquitas and other naturally rare endangered
42 species and highlights the utility of genomics in predicting extinction risk.

43

44 **One-sentence summary:** Whole genome sequencing and genomics-based population viability
45 analyses suggest the vaquita is not doomed to extinction.

46

47 **Main Text:**

48 A central question for populations that have undergone severe declines is whether recovery is
49 possible, or if it may be hindered by deleterious genetic factors (1). Perhaps the most
50 immediate genetic threat in populations of very small size (<25 individuals) is the deterioration
51 of fitness due to inbreeding depression (2, 3). Thus, predicting the threat of inbreeding
52 depression under various genetic and demographic conditions is essential for the conservation
53 of endangered species.

54

55 The critically endangered vaquita porpoise (*Phocoena sinus*), found only in the northernmost
56 Gulf of California, Mexico, has declined from ~600 individuals in 1997 to around 10 individuals
57 at present (4). This precipitous decline has been driven by incidental mortality in fishing gillnets
58 (bycatch) ((4, 5); Fig. 1A). Efforts to reduce the intensity of illegal gillnet fishing and implement
59 stronger protections for vaquitas have not been successful, and vaquitas are now considered
60 the most endangered marine mammal (4). A recent viability analysis found that the vaquita
61 population could theoretically rebound if bycatch mortality is eliminated (6). However, the
62 degree to which genetic factors may prevent a robust recovery is unknown, leading some to
63 argue that the species is doomed to extinction from genetic threats (see discussion in (1, 7, 8)).

64

65 Population viability analysis (PVA) has long been an important tool for modelling extinction risk
66 (9). However, it is often challenging to parameterize PVA models for highly endangered species
67 where information on the potential impact of inbreeding depression is limited. Genomic data
68 offer a potential solution, as they can be used to estimate the fundamental genetic and
69 demographic parameters underlying inbreeding depression. Although the potential applications
70 of genomics in conservation have been widely discussed (10, 11), genomics remain under-
71 utilized in forecasts of population viability and extinction risk.

72

73 To investigate the impact of the vaquita's recent decline and to quantify the species' recovery
74 potential, we sequenced genomic DNA of 19 archival tissue samples to high depth (total n = 20
75 including genome from (12), mean coverage = 60X; table S1). Samples were obtained across

76 three time periods: 1985-1993, 2004, and 2016-2017, spanning ~3 vaquita generations
77 (assuming a generation time of 11.9 years; (13)) and an estimated ~99% decline in population
78 size (Fig. 1A, (5)). All 20 vaquita genomes contain uniformly low heterozygosity (mean =
79 9.04×10^{-5} , standard deviation (S.D.) = 2.44×10^{-6} heterozygotes/site; Fig. 1B and fig. S1),
80 consistent with a previous estimate from a single individual (12). Additionally, genome-wide
81 diversity appears stable over the sampling period (Fig. 1B, C), as expected given the short
82 duration of the decline.

83

84 We also investigated whether vaquita genomes show signs of recent inbreeding. We found that
85 the mean cumulative fraction of vaquita genomes in long (≥ 1 Mb) runs of homozygosity (ROH)
86 is 5.42% (S.D. = 1.7%), implying a low average inbreeding coefficient of $F_{\text{ROH}} = 0.05$ (Fig. 1D and
87 fig. S2). Furthermore, ROH in our sample are relatively short (mean length 1.59-3.18 Mb),
88 suggesting that they trace to a common ancestor from roughly 15-31 generations ago (178-369
89 years; (5)). This result indicates that these ROH are a consequence of the vaquita's historically
90 limited population size rather than recent inbreeding. Finally, we found limited evidence for
91 close relatives in our dataset, aside from two known mother-fetus pairs (fig. S3).

92

93 To better characterize the vaquita's long-term demographic history, we used the distribution of
94 allele frequencies to perform model-based demographic inference. Overall, we found good fit
95 for a two-epoch model in which the vaquita effective population size (N_e) declined from 4,485
96 to 2,807 individuals ~2,162 generations ago (~25.7 KYA; (5); Fig. 1E, figs. S4 and S5, tables S2 to
97 S4). Thus, vaquitas have persisted at relatively small population sizes for at least tens of
98 thousands of years, resulting in uniformly low genome-wide diversity that is among the lowest
99 documented in any species to date (12). Here, we use 'long-term small population size' to mean
100 N_e on the order of a few thousand individuals over thousands of generations, as opposed to
101 'small population size' meaning $N_e \leq 100$, as in some other contexts (e.g., (14, 15)).

102

103 A predicted consequence of long-term small population size is the reduced efficacy of purifying
104 selection against weakly deleterious alleles with selection coefficients $\ll 1/(2 * N_e)$ (14, 15). Such

105 alleles can drift to high frequencies and become fixed, potentially contributing to reduced
106 fitness. To investigate this, we compared the burden of putatively deleterious protein-coding
107 variants in vaquitas with 11 other cetacean species (table S5, fig. S6). Specifically, we focused
108 on nonsynonymous mutations at sites under strong evolutionary constraint (16), and loss-of-
109 function (LOF) mutations that are predicted to disrupt gene function. We used the ratio of
110 deleterious to synonymous variants as a proxy for the efficacy of purifying selection (5) and
111 used genome-wide heterozygosity as a proxy for N_e (Fig. 2A, B and fig. S7). The ratio of
112 deleterious variants is significantly negatively correlated with N_e (phylogenetic generalized least
113 squares (PGLS) regression, $p_{\text{del.}} = 1.32 \times 10^{-2}$, $p_{\text{LOF}} = 7.88 \times 10^{-3}$), consistent with expectation.
114 Among all species in our study, vaquitas have the highest proportional burden of deleterious
115 alleles. Compared to the species with the next lowest diversity (orca, *Orcinus orca*), ratios for
116 deleterious and LOF mutations in vaquitas are 1.14x and 1.23x higher, respectively.
117 Furthermore, we demonstrate using simulations that this elevated ratio is minimally impacted
118 by the vaquita's recent population decline, and is instead attributable to its historical
119 population size (fig. S9; (5)). Similar trends exist for homozygous deleterious mutations, which
120 includes variants that may be fixed in the species (fig. S8). Thus, elevated ratios of deleterious
121 to neutral variation among polymorphisms (heterozygotes) and substitutions (homozygotes) in
122 vaquitas are consistent with an accumulation of weakly deleterious alleles under long-term
123 small population size. The remaining vaquita individuals appear healthy and are actively
124 reproducing (17, 18), suggesting the species' fitness has not been severely compromised by its
125 longstanding elevated burden of weakly deleterious alleles.

126

127 A larger concern for vaquita recovery is future fitness declines due to inbreeding depression,
128 given the inevitability of inbreeding in any recovery scenario. However, the risk of inbreeding
129 depression (or "inbreeding load") is predicted to be reduced in species with long-term small
130 population size because 1) increased homozygosity exposes recessive strongly deleterious
131 alleles to selection more frequently, and 2) drift decreases the absolute number of segregating
132 recessive deleterious variants (19, 20). To assess the potential for future inbreeding depression
133 in vaquitas relative to other cetaceans, we quantified the total number of heterozygous

134 deleterious alleles per genome, which reflect alleles that could contribute to inbreeding
135 depression when made homozygous through inbreeding. We found that the total number of
136 heterozygous putatively deleterious alleles per genome is positively correlated with genome-
137 wide diversity (PGLS $p_{\text{del.}} = 5.57 \times 10^{-6}$, $p_{\text{LOF}} = 1.91 \times 10^{-5}$) (Fig. 2C, D). Among all cetaceans in our
138 study, vaquitas harbor the fewest deleterious heterozygotes per genome. Compared to the
139 orca, vaquitas have 0.33x and 0.36x the number of deleterious and LOF heterozygotes,
140 respectively. Similar trends are evident in all mutation classes, including conserved noncoding
141 regions (fig. S10). Thus, although vaquitas have an elevated proportion of deleterious relative to
142 neutral variants (Fig. 2A, B, fig. S8), they nevertheless have a low absolute number of
143 segregating deleterious variants (Fig. 2C, D), implying a low inbreeding load.

144

145 To model potential recovery scenarios for the vaquita, we combined our genomic results with
146 information about vaquita life history to parameterize stochastic, individual-based simulations
147 using SLiM3 ((5, 21); Fig. 3A, fig. S11). These simulations were designed to model vaquita
148 protein-coding regions, incorporating both neutral mutations and recessive deleterious
149 mutations, the latter of which are thought to underlie inbreeding depression (3, 22). We used
150 our genomic dataset to estimate a vaquita mutation rate (fig. S12) as well as a distribution of
151 selection coefficients for new mutations (fig. S13), and assumed an inverse relationship
152 between dominance and selection coefficients (5). Importantly, our model allows for
153 deleterious mutations to drift to fixation and impact fitness (figs. S14 to S16; (5)). We used our
154 demographic model (Fig. 1E) to simulate the historical vaquita population (figs. S17 and S18),
155 then initiated a bottleneck by introducing stochastic bycatch mortality at a rate calibrated to
156 the empirical rate of recent decline as of 2018 (Fig. 1A and fig. S19; (5)). Finally, we allowed for
157 recovery by reducing the bycatch mortality rate after the population reached a 'threshold
158 population size' of 10 or fewer individuals, based on the current estimated population size.

159

160 We first used this model to examine the impact of varying levels of bycatch mortality on
161 extinction risk over the next 50 years. We estimate a high probability of recovery if bycatch
162 mortality ceases entirely, with only 6% of simulation replicates going extinct (Figs. 3B, 4A). In

163 addition, simulated populations that persist exhibit substantial growth, with a mean population
164 size in 2070 of 298.7 individuals (S.D. = 218.2; Fig. 4A). However, if bycatch mortality rates are
165 decreased by just 90%, extinction rates increase to 27% (Figs. 3B and 4B), with more limited
166 recovery in population sizes (mean of 49.2 individuals in 2070, S.D. = 34.4; Fig. 4B). Finally, if
167 bycatch mortality rates are decreased by just 80%, extinction occurs in 62% of simulation
168 replicates. Thus, recovery potential critically depends on reducing bycatch mortality rates, with
169 even moderate levels of bycatch resulting in a high likelihood of extinction.

170

171 Next, we examined the importance of the threshold population size, given uncertainty in the
172 2018 estimate of 10 individuals (4). As expected, extinction rates decrease when assuming a
173 threshold population size of 20 and increase when assuming a threshold population size of 5
174 (Fig. 3B). These results emphasize that the number of remaining vaquita individuals is also a
175 critical factor underlying extinction risk.

176

177 To quantify the inbreeding load in our model, we estimated the ‘number of diploid lethal
178 equivalents’ (or $2B$), which characterizes the rate at which fitness is lost with increasing levels of
179 inbreeding (2, 23). Typically, inbreeding load is quantified by comparing estimates of individual
180 fitness and inbreeding in natural populations (2, 24); however, such data do not exist for most
181 species, including the vaquita. Under our simulation parameters, we estimate an inbreeding
182 load of $2B = 0.95$ in vaquitas (table S6), significantly lower than the median empirical estimate
183 for mammals of 6.2 (24), likely due to the vaquita’s relatively small historical N_e . Nevertheless,
184 simulations that exclude deleterious mutations result in a significantly lower extinction rate
185 (Fig. 3B), confirming that inbreeding depression impacts recovery potential in our model.

186

187 To further explore how the inbreeding load in our model depends on historical demography, we
188 ran simulations with the historical N_e increased x20. We found an increased extinction rate of
189 52%, compared to 27% with our empirical population size parameters, with minimal recovery
190 for replicates that persisted (mean of 16.2 individuals in 2070, S.D. = 14.5, Fig. 4C). Additionally,
191 with this larger historical N_e , we observe a greatly increased inbreeding load of $2B = 3.32$ (fig.

192 S20 and table S6). These findings further demonstrate the importance of the vaquita's natural
193 rarity as a factor underlying their low inbreeding load and increased potential for recovery.

194

195 Given the uncertainty in many of our model parameters, we conducted sensitivity analyses
196 varying the calving interval, mutation rate, distribution of dominance and selection coefficients,
197 and target size for deleterious mutations (5). Although these factors influence extinction
198 probabilities, recovery remains the likely outcome (>50% probability) in nearly all cases when
199 assuming a threshold population size of 10 and a 90% reduction of bycatch mortality (fig. S21
200 and table S6). Two notable exceptions to this are for models with a higher mutation rate, where
201 we observed a 55% extinction rate compared to 27% in our 'base' model, and for models with
202 decreased calving interval, where we also observed a 55% extinction rate (fig. S21 and table S6).
203 Thus, although uncertainty exists in our projections, the overall conclusion that recovery is
204 possible if bycatch is greatly reduced remains robust to our model assumptions. Finally, we
205 note that our simulations do not consider factors such as reduced adaptive potential or
206 increased susceptibility to disease caused by low genetic variability, which may impact future
207 persistence. Vaquitas have survived with low diversity for tens of thousands of years and have
208 endured environmental changes in the past (12), suggesting that these factors alone do not
209 doom the species to extinction. Conceivably, low diversity in the vaquita may limit the species'
210 capacity to adapt to increasing global change over the long term, but this risk is challenging to
211 quantify and should not preclude recovery efforts in the short term.

212

213 In conclusion, our results suggest there is a high potential for vaquita recovery in the absence of
214 gillnet mortality, refuting the view that the species is doomed to extinction by genetic factors.
215 Our approach leverages genomic data and methodology to forecast population viability and
216 extinction risk, enabling a more nuanced assessment of the threat of genetic factors to
217 persistence. The key aspect of the vaquita that our analysis reveals is that its historical
218 population size was large enough to prevent the fixation of all but weakly deleterious alleles,
219 and small enough to reduce the inbreeding load from recessive strongly deleterious mutations.
220 Numerous other examples of species rebounding from bottlenecks of similar magnitude to that

221 of the vaquita have been documented (reviewed in (1)). For example, many parallels exist
222 between the vaquita and Channel Island foxes, which similarly have exceptionally low genetic
223 diversity, yet were able to rebound from severe recent bottlenecks without apparent signs of
224 inbreeding depression (25). Together, these examples challenge the assumption that
225 populations that have experienced catastrophic declines are genetically doomed and provide
226 hope for the recovery of endangered species that are naturally rare. Finally, our analysis
227 demonstrates the potential for genomics-informed population viability modelling, which may
228 have widespread applications given the increasing feasibility of genomic sequencing for non-
229 model species amid a worsening extinction crisis (26).

230

231 **References and Notes**

- 232 1. D. A. Wiedenfeld *et al.*, *Conserv. Biol.* **35**, 1388–1395 (2021).
- 233 2. L. Keller, D. M. Waller, *Trends Ecol. Evol.* **17**, 19–23 (2002).
- 234 3. D. Charlesworth, J. H. Willis, *Nat. Rev. Genet.* **10**, 783–796 (2009).
- 235 4. A. M. Jaramillo-Legorreta *et al.*, *R. Soc. Open Sci.* **6** (2019), doi:10.1098/rsos.190598.
- 236 5. *Materials and methods and supplementary text are available as supplementary*
- 237 *materials.*
- 238 6. M. A. Cisneros-Mata, J. A. Delgado, D. Rodríguez-Félix, *Rev. Biol. Trop.* **69**, 588–600
- 239 (2021).
- 240 7. B. L. Taylor, L. Rojas-Bracho, *Mar. Mammal Sci.* **15**, 1004–1028 (1999).
- 241 8. C. Sonne, P. Diaz-Jaimes, D. H. Adams, *Science (80-)*. **373**, 863–864 (2021).
- 242 9. B. W. Brook *et al.*, *Nature*. **404**, 385–387 (2000).
- 243 10. F. W. Allendorf, P. A. Hohenlohe, G. Luikart, *Nat. Rev. Genet.* **11**, 697–709 (2010).
- 244 11. H. A. Lewin *et al.*, *Proc. Natl. Acad. Sci. U. S. A.* **115**, 4325–4333 (2018).
- 245 12. P. A. Morin *et al.*, *Mol. Ecol. Resour.* **21**, 1008–1020 (2021).
- 246 13. B. L. Taylor, S. J. Chivers, J. Larese, W. F. Perrin, “Generation length and percent mature
- 247 estimates for IUCN assessments of cetaceans” (2007).
- 248 14. M. Lynch, I. J. Conery, R. Burger, *Am. Nat.* **146**, 489–518 (1995).
- 249 15. M. Kimura, T. Maruyama, J. F. Crow, *Genetics*, 1303–1312 (1963).
- 250 16. P. C. Ng, S. Henikoff, *Genome Res.* **11**, 863–874 (2001).
- 251 17. B. L. Taylor *et al.*, *Mar. Mammal Sci.* **35**, 1603–1612 (2019).
- 252 18. F. Gulland *et al.*, *Vet. Rec.* **187**, 1–4 (2020).
- 253 19. C. C. Kyriazis, R. K. Wayne, K. E. Lohmueller, *Evol. Lett.* **5**, 33–47 (2021).
- 254 20. S. Glémin, *Evolution (N. Y.)*. **57**, 2678–2687 (2003).
- 255 21. B. C. Haller, P. W. Messer, *Mol. Biol. Evol.* **36**, 632–637 (2019).
- 256 22. A. R. McCune *et al.*, *Science (80-)*. **296**, 2398–2401 (2002).
- 257 23. N. E. Morton, J. F. Crow, H. J. Muller, *Proc. Natl. Acad. Sci.* **42**, 855–863 (1956).
- 258 24. K. Ralls, J. D. Ballou, A. Templeton, K. Ralls, J. D. Ballou, *Soc. Conserv. Biol.* **2**, 185–193
- 259 (1988).
- 260 25. J. A. Robinson, C. Brown, B. Y. Kim, K. E. Lohmueller, R. K. Wayne, *Curr. Biol.* **28**, 3487–
- 261 3494.e4 (2018).
- 262 26. G. Ceballos, P. R. Ehrlich, P. H. Raven, *Proc. Natl. Acad. Sci. U. S. A.* **117**, 13596–13602
- 263 (2020).
- 264 27. Scripts for sequence data processing, (available at doi:10.5281/zenodo.6303135).
- 265 28. Scripts for simulations, (available at doi:10.5281/zenodo.6303135).
- 266 29. S. A. Miller, D. D. Dykes, H. F. Polesky, *Nucleic Acids Res.* **16**, 1215 (1988).
- 267 30. M. Meyer, M. Kircher, *Cold Spring Harb. Protoc.* **5** (2010), doi:10.1101/pdb.prot5448.
- 268 31. M. Kircher, S. Sawyer, M. Meyer, *Nucleic Acids Res.* **40**, 1–8 (2012).
- 269 32. G. A. Van der Auwera *et al.*, *Curr. Protoc. Bioinforma.*, 1–33 (2013).
- 270 33. H. Li, *arXiv:1303.3997v2*. **00**, 1–3 (2013).
- 271 34. H. Li, *Bioinformatics*. **27**, 2987–2993 (2011).
- 272 35. A. Smit, R. Hubley, P. Green, RepeatMasker Open-4.0 2013-2015, (available at
- 273 <http://www.repeatmasker.org>).
- 274 36. G. Benson, *Nucleic Acids Res.* **27**, 573–580 (1999).

- 275 37. A. M. Jaramillo-Legorreta, L. Rojas-Bracho, T. Gerrodette, *Mar. Mammal Sci.* **15**, 957–973
276 (1999).
- 277 38. T. Gerrodette *et al.*, *Mar. Mammal Sci.* **27**, 79–100 (2011).
- 278 39. B. L. Taylor *et al.*, *Conserv. Lett.* **10**, 588–595 (2017).
- 279 40. C. C. Chang *et al.*, *Gigascience.* **4**, 1–16 (2015).
- 280 41. P. Danecek *et al.*, *Bioinformatics.* **27**, 2156–2158 (2011).
- 281 42. V. Narasimhan *et al.*, *Bioinformatics.* **32**, 1749–1751 (2016).
- 282 43. S. R. Browning, *Genetics.* **178**, 2123–2132 (2008).
- 283 44. A. Manichaikul *et al.*, *Bioinformatics.* **26**, 2867–2873 (2010).
- 284 45. X. Zheng *et al.*, *Bioinformatics.* **28**, 3326–3328 (2012).
- 285 46. C. Camacho *et al.*, *BMC Bioinformatics.* **10**, 421 (2009).
- 286 47. R. N. Gutenkunst, R. D. Hernandez, S. H. Williamson, C. D. Bustamante, *PLoS Genet.* **5**, 1–
287 11 (2009).
- 288 48. L. Excoffier, I. Dupanloup, E. Huerta-Sánchez, V. C. Sousa, M. Foll, *PLOS Genet.* **9**,
289 e1003905 (2013).
- 290 49. A. J. Coffman, P. H. Hsieh, S. Gravel, R. N. Gutenkunst, *Mol. Biol. Evol.* **33**, 591–593
291 (2016).
- 292 50. A. Dornburg, M. C. Brandley, M. R. McGowen, T. J. Near, *Mol. Biol. Evol.* **29**, 721–736
293 (2012).
- 294 51. M. Autenrieth *et al.*, *Mol. Ecol. Resour.* **18**, 1469–1481 (2018).
- 295 52. H.-S. Yim *et al.*, *Nat. Genet.* **46**, 88–92 (2014).
- 296 53. Y. Ben Chehida *et al.*, *Sci. Rep.* **10**, 1–18 (2020).
- 297 54. S. Kumar, G. Stecher, M. Suleski, S. B. Hedges, *Mol. Biol. Evol.* **34**, 1812–1819 (2017).
- 298 55. C. Feng *et al.*, *Elife.* **6**, 1–14 (2017).
- 299 56. F. L. Wu *et al.*, *PLoS Biol.* **18**, 1–38 (2020).
- 300 57. R. Vaser, S. Adusumalli, S. N. Leng, M. Sikic, P. C. Ng, *Nat. Protoc.* **11**, 1–9 (2016).
- 301 58. P. Cingolani *et al.*, *Fly (Austin).* **6**, 80–92 (2012).
- 302 59. D. MacArthur, S. Balasubramanian, A. Frankish, *Science (80-.).* **335**, 1–14 (2012).
- 303 60. B. M. Henn, L. R. Botigué, C. D. Bustamante, A. G. Clark, S. Gravel, *Nat. Rev. Genet.* **16**,
304 333–343 (2015).
- 305 61. Y. Brandvain, S. I. Wright, *Trends Genet.* **32**, 201–210 (2016).
- 306 62. R. Do *et al.*, *Nat. Genet.* **47**, 126–131 (2015).
- 307 63. M. Seppey, M. Manni, E. M. Zdobnov, *BUSCO: Assessing genome assembly and*
308 *annotation completeness* (2019), vol. 1962.
- 309 64. K. Katoh, D. M. Standley, *Mol. Biol. Evol.* **30**, 772–780 (2013).
- 310 65. B. Q. Minh *et al.*, *Mol. Biol. Evol.* **37**, 1530–1534 (2020).
- 311 66. B. D. Rosen *et al.*, *Gigascience.* **9**, 1–9 (2020).
- 312 67. S. Capella-Gutiérrez, J. M. Silla-Martínez, T. Gabaldón, *Bioinformatics.* **25**, 1972–1973
313 (2009).
- 314 68. C. Creevy, catsequences: A tool for concatenating multiple fasta alignments for
315 supermatrix phylogenetic analyses, (available at doi: 10.5281/zenodo.4409153).
- 316 69. O. Chernomor, A. Von Haeseler, B. Q. Minh, *Syst. Biol.* **65**, 997–1008 (2016).
- 317 70. S. Kalyaanamoorthy, B. Q. Minh, T. K. F. Wong, A. Von Haeseler, L. S. Jermini, *Nat.*
318 *Methods.* **14**, 587–589 (2017).

- 319 71. M. R. McGowen *et al.*, *Syst. Biol.* **69**, 479–501 (2020).
- 320 72. D. T. Hoang, O. Chernomor, A. Von Haeseler, B. Q. Minh, L. S. Vinh, *Mol. Biol. Evol.* **35**,
- 321 518–522 (2018).
- 322 73. R Core Team, R: A language and environment for statistical computing. (2021), (available
- 323 at <https://www.r-project.org/>).
- 324 74. E. Paradis, K. Schliep, *Bioinformatics.* **35**, 526–528 (2019).
- 325 75. M. W. Pennell *et al.*, *Bioinformatics.* **30**, 2216–2218 (2014).
- 326 76. J. Pinheiro, D. Bates, S. DebRoy, D. Sarkar, nlme: Linear and Nonlinear Mixed Effects
- 327 Models. R package version 3.1-152, (available at [https://cran.r-](https://cran.r-project.org/package=nlme)
- 328 [project.org/package=nlme](https://cran.r-project.org/package=nlme)).
- 329 77. D. Polychronopoulos, J. W. D. King, A. J. Nash, G. Tan, B. Lenhard, *Nucleic Acids Res.* **45**,
- 330 12611–12624 (2017).
- 331 78. A. Siepel *et al.*, *Genome Res.* **15**, 1034–1050 (2005).
- 332 79. C. D. Huber, B. Y. Kim, C. D. Marsden, K. E. Lohmueller, *Proc. Natl. Acad. Sci.* **114**, 4465–
- 333 4470 (2017).
- 334 80. B. Y. Kim, C. D. Huber, K. E. Lohmueller, *Genetics.* **206**, 345–361 (2017).
- 335 81. D. Castellano, M. C. Macià, P. Tataru, T. Bataillon, K. Munch, *Genetics.* **213**, 953–966
- 336 (2019).
- 337 82. J. E. Moore, A. J. Read, *Ecol. Appl.* **18**, 1914–1931 (2008).
- 338 83. J. A. Robinson *et al.*, *Sci. Adv.* **5**, 1–13 (2019).
- 339 84. P. W. Hedrick, A. Garcia-Dorado, *Trends Ecol. Evol.* **31**, 940–952 (2016).
- 340 85. M. Kardos *et al.*, *Proc. Natl. Acad. Sci. U. S. A.* **118**, 1–10 (2021).
- 341 86. Z. Gao, D. Waggoner, M. Stephens, C. Ober, M. Przeworski, *Genetics.* **199**, 1243–1254
- 342 (2015).
- 343 87. B. Charlesworth, *Evolution in age-structured populations* (Cambridge University Press,
- 344 1994).
- 345 88. K. S. Norris, J. . Prescott, *Univ. Calif. Publ. Zool.* **63**, 291–402 (1961).
- 346 89. E. Mitchell, *J. Fish. Res. Board Canada.* **32**, 889–983 (1975).
- 347 90. O. Vidal, in *Biology of the Phocoenids. Reports of the International Whaling Commission*
- 348 *(Special Issue 16)*. (Cambridge, UK., 1995), pp. 247–272.
- 349 91. C. D’Agrosa, C. E. Lennert-Cody, O. Vidal, *Conserv. Biol.* **14**, 1110–1119 (2000).
- 350 92. A. A. Hohn, A. J. Read, S. Fernandez, O. Vidal, L. T. Findley, *J. Zool.* (1996).
- 351 93. T. Gerrodette, L. Rojas-Bracho, *Mar. Mammal Sci.* **27**, 101–125 (2011).
- 352 94. L. Rojas-Bracho, R. R. Reeves, A. Jaramillo-Legorreta, *Mamm. Rev.* **36**, 179–216 (2006).
- 353 95. M. Lynch, J. Conery, R. Burger, *Evolution (N. Y.)*. **49**, 1067–1080 (1995).
- 354 96. M. Lynch, W. Gabriel, *Evolution (N. Y.)*. **44**, 1725–1737 (1990).
- 355 97. G. R. Warnes *et al.*, gplots: Various R Programming Tools for Plotting Data. R package
- 356 version 3.1.1 (2020), (available at <https://cran.r-project.org/package=gplots>).
- 357 98. S. J. M. Jones *et al.*, *Genes (Basel)*. **8** (2017), doi:10.3390/genes8120378.
- 358 99. Ú. Árnason, F. Lammers, V. Kumar, M. A. Nilsson, A. Janke, (2018).
- 359 100. X. Zhou *et al.*, *Nat. Commun.* **9**, 1–8 (2018).
- 360 101. A. D. Foote *et al.*, *Nat. Genet.* **47**, 272–275 (2015).
- 361 102. A. E. Moura *et al.*, *Mol. Biol. Evol.* **31**, 1121–1131 (2014).
- 362 103. M. V. Westbury, B. Petersen, E. Garde, M. P. Heide-Jørgensen, E. D. Lorenzen, *iScience.*

- 363 **15**, 592–599 (2019).
- 364 104. G. Fan *et al.*, *Mol. Ecol. Resour.* **19**, 944–956 (2019).
- 365 105. W. C. Warren *et al.*, *Genome Biol. Evol.* **9**, 3260–3264 (2017).
- 366 106. Y. Yuan *et al.*, *Genes (Basel)*. **9**, 1–9 (2018).
- 367

368 **Acknowledgments**

369 We thank the CanSeq150 project for use of the long-finned pilot whale and Pacific white-sided
370 dolphin genomes. Y. Bukhman generously provided early access to the blue whale genome. We
371 thank J. Mah, P. Nuñez, and M. Lin for providing scripts, and B. Haller for assistance with
372 simulations. We thank the Southwest Fisheries Science Center’s Marine Mammal and Sea Turtle
373 Research Collection for use of archival vaquita tissue samples. All samples were imported to the
374 US under appropriate CITES and US Marine Mammal Protection Act permits. **Funding:** We thank
375 Frances Gulland, The Marine Mammal Center, and NOAA Fisheries for funding genome
376 resequencing. C.C.K. and K.E.L. were supported by National Institutes of Health (NIH) grant
377 R35GM119856 (to K.E.L.). A.C.B. was supported by the Biological Mechanisms of Healthy Aging
378 Training Program NIH T32AG066574. S.N.M. was supported by the Mexican National Council for
379 Science and Technology (CONACYT) Postdoctoral Fellowship 724094 and the Mexican
380 Secretariat of Agriculture and Rural Development Postdoctoral Fellowship. **Author**
381 **contributions:** P.A.M., B.L.T., J.A.R. and C.C.K. designed the study. P.A.M., M.C.F., L.R.B. and
382 B.L.T obtained funding. P.A.M., B.L.T., and L.R.B. obtained samples. K.M.R. performed DNA
383 extractions and library preparations. A.C.B., S.F.N.M, J.A.R., and C.C.K. performed analyses.
384 J.A.R. and C.C.K. wrote the manuscript with input from all authors. P.A.M., B.L.T., K.E.L., and
385 R.K.W. supervised the work. **Competing interests:** The authors declare no competing interests.
386 **Data and materials availability:** Vaquita raw sequence reads have been deposited in the
387 Sequence Read Archive (SRA) under BioProject PRJNA751981 (see table S1 for details).
388 Accession information for publicly available cetacean genomes is provided in table S5. Scripts
389 used for sequence data processing and analysis are available at doi:10.5281/zenodo.6303135.
390 Scripts for simulations are available at doi:10.5281/zenodo.6308771.
391

392 **Figure Legends**

393 **Fig. 1. Vaquita genome-wide diversity and demographic history.** (A) Model of vaquita census
394 population size based on previous surveys (5) shows a dramatic recent decline. (B) Bar plots of
395 per-site heterozygosity in 1-Mb genomic windows in three individuals (one from each sampling
396 period; see fig. S1 for all) show little variability within or between individuals. (C, D) Genome-
397 wide heterozygosity and ROH burden are consistent between sampling periods. Lines connect
398 mother-fetus pairs; open symbols indicate offspring. (E) Two-epoch demographic model
399 inferred with $\partial a \partial i$. Parameter 95% confidence intervals indicated in parentheses.

400

401 **Fig. 2. Deleterious variation in vaquitas and other cetaceans.** Ratios of deleterious
402 nonsynonymous (A) and LOF (B) heterozygotes to synonymous heterozygotes are significantly
403 negatively correlated with genome-wide heterozygosity (per bp, log-scaled). Total numbers of
404 deleterious nonsynonymous (C) and LOF (D) heterozygotes per genome are significantly
405 positively correlated with genome-wide heterozygosity (per bp). Grey lines show phylogeny-
406 corrected regressions (excluding the Indo-Pacific finless porpoise (5)).

407

408 **Fig. 3. Model schematic and extinction rates under various simulation parameters.** (A)
409 Diagram of events that occur during one year in our SLiM simulation model. (B) Percent of
410 replicates going extinct over the next 50 years under varying recovery parameters. Shading
411 indicates extinction rates when only neutral mutations are simulated, and “N” represents the
412 threshold population size.

413

414 **Fig. 4. Simulation trajectories under various recovery scenarios.** (A) Simulation trajectories
415 under empirically-inferred historical demographic parameters assuming a reduction in bycatch
416 mortality of 100%. (B) Simulation trajectories with bycatch mortality rate decreased by only
417 90%. (C) Simulation trajectories with historical population size increased x20 and assuming a
418 decrease in bycatch mortality of 90%. For all simulations, we assumed a population size
419 threshold of 10 individuals. Replicates that went extinct are colored red and replicates that
420 persisted are colored blue.

421

422 **Supplementary Materials**

423 Materials and Methods

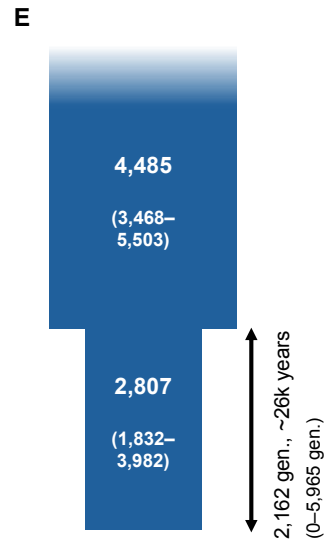
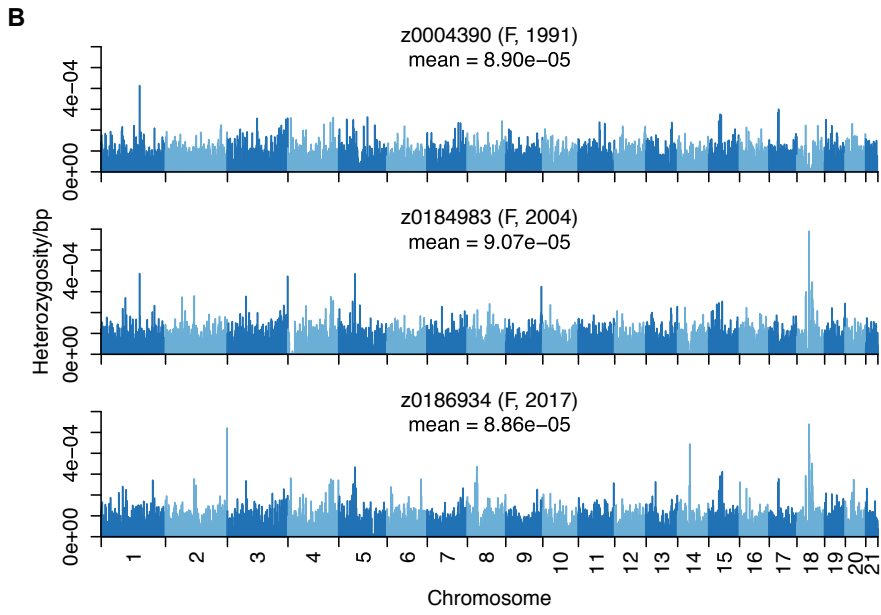
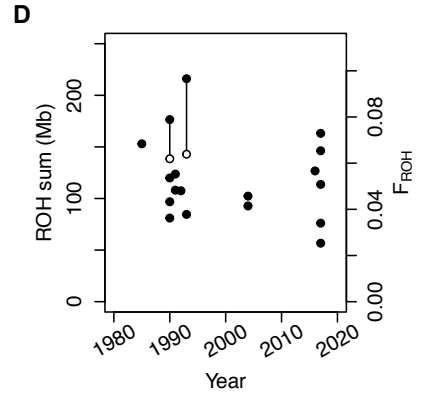
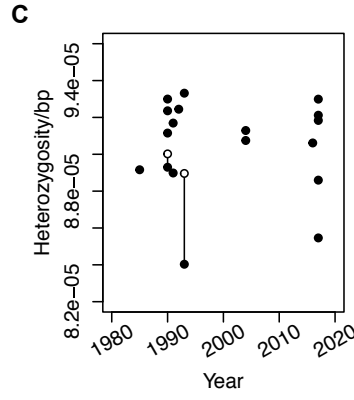
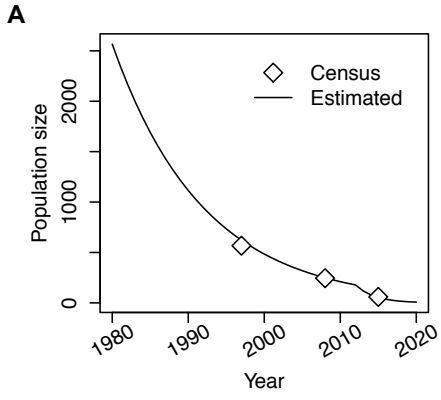
424 Supplementary Text

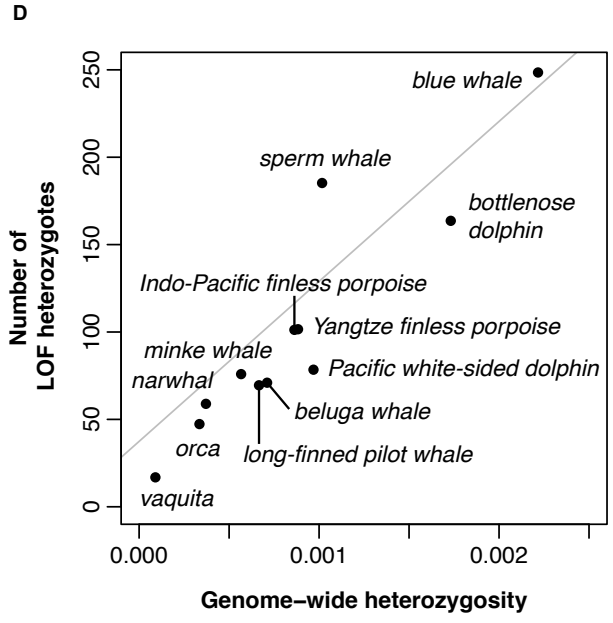
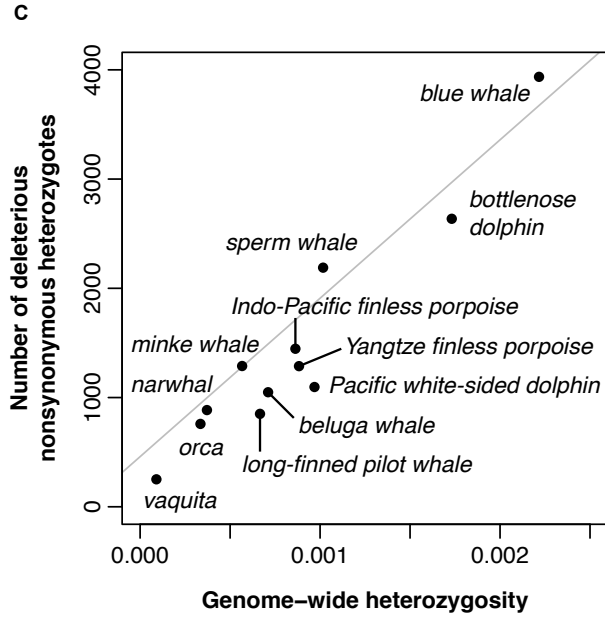
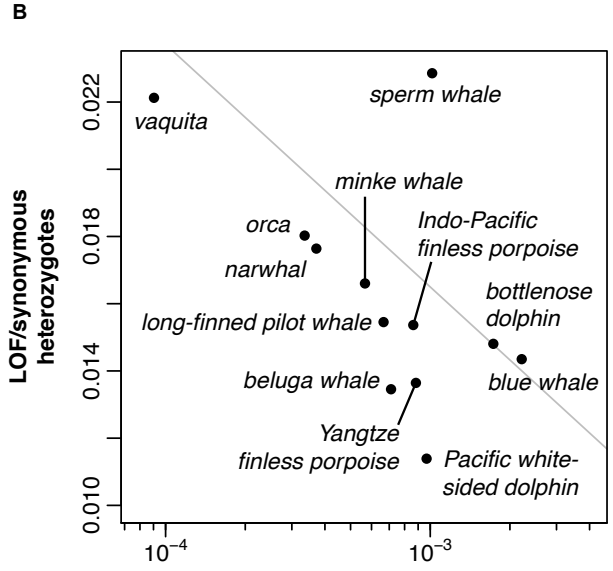
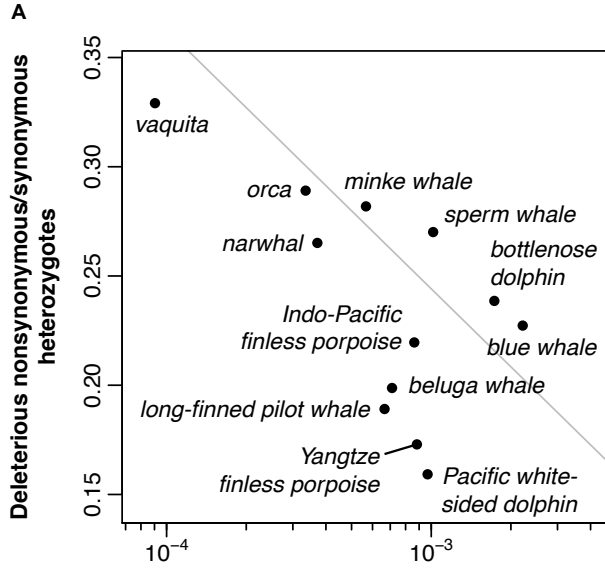
425 Tables S1 to S6

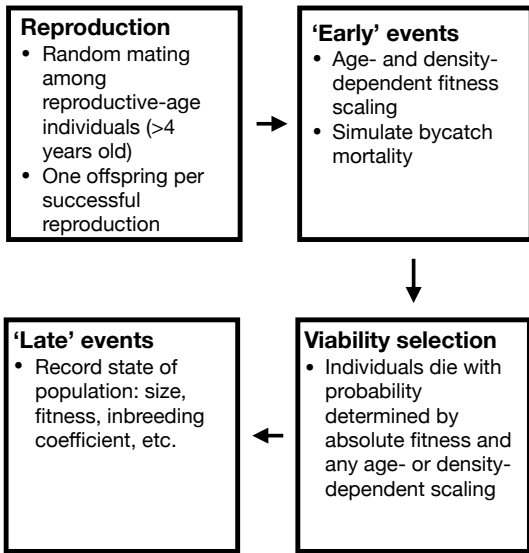
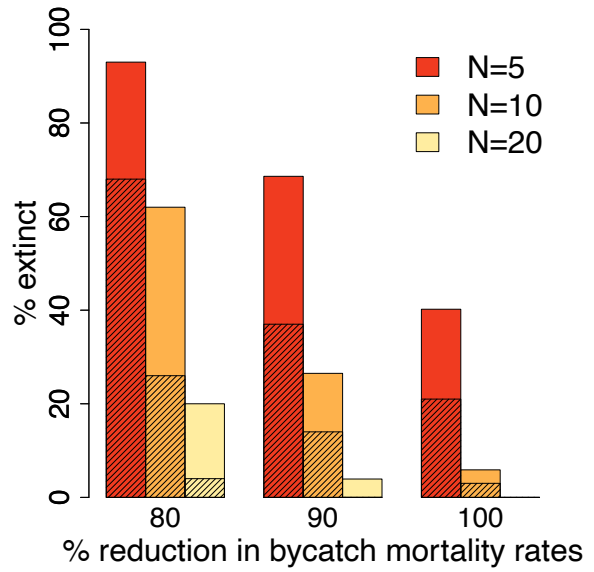
426 Figs. S1 to S21

427

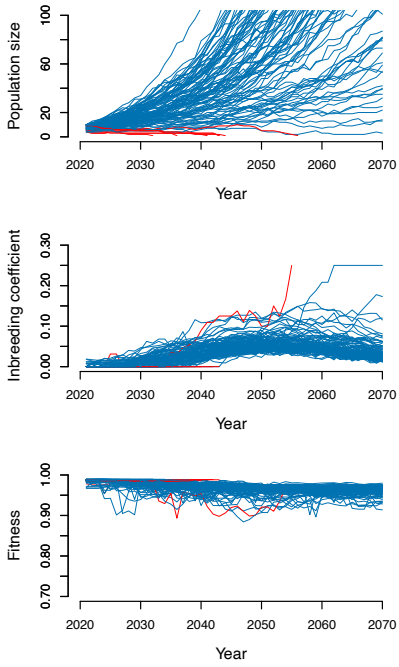
428



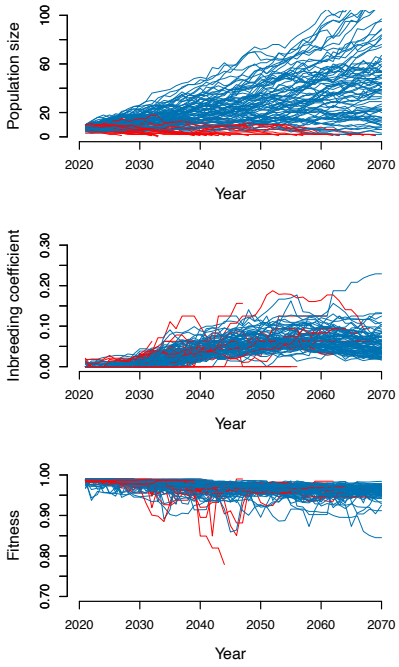


A**B**

A 100% reduction in bycatch mortality rates
($2B=0.95$; 6% extinct)



B 90% reduction in bycatch mortality rates
($2B=0.95$; 27% extinct)



C 90% reduction in bycatch mortality rates,
historical population size increased x20
($2B=3.32$; 52% extinct)

